Dynamic force spectroscopy of DNA hairpins: I. Force kinetics and free energy landscapes

J. Stat. Mech. (2009) P02060

(http://iopscience.iop.org/1742-5468/2009/02/P02060)

Journal of Statistical Mechanics: Theory and Experiment
An IOP and SISSA journal

Dynamic force spectroscopy of DNA hairpins: I. Force kinetics and free energy landscapes

A Mossa[1], M Manosas[1,3], N Forns[1,2], J M Huguet[1] and F Ritort[1,2]

[1] Departament de Física Fonamental, Facultat de Física, Universitat de Barcelona, Diagonal 647, Barcelona 08028, Spain
[2] CIBER-BBN Networking Centre on Bioengineering, Biomaterials and Nanomedicine, Spain
E-mail: alessandro.mossa@gmail.com, mmanosas@gmail.com, nuforns@ub.edu, johuca@yahoo.com and ritort@ffn.ub.es

Received 9 December 2008
Accepted 17 January 2009
Published 25 February 2009

Online at stacks.iop.org/JSTAT/2009/P02060
doi:10.1088/1742-5468/2009/02/P02060

Abstract. We investigate the thermodynamics and kinetics of DNA hairpins that fold/unfold under the action of applied mechanical force. We introduce the concept of the molecular free energy landscape and derive simplified expressions for the force dependent Kramers–Bell rates. To test the theory we have designed a specific DNA hairpin sequence that shows two-state cooperative folding under mechanical tension and carried out pulling experiments using optical tweezers. We show how we can determine the parameters that characterize the molecular free energy landscape of such sequences from rupture force kinetic studies. Finally we combine such kinetic studies with experimental investigations of the Crooks fluctuation relation to derive the free energy of formation of the hairpin at zero force.

Keywords: fluctuations (theory), fluctuations (experiment), mechanical properties (DNA, RNA, membranes, bio-polymers) (theory), mechanical properties (DNA, RNA, membranes, bio-polymers) (experiment)

[3] Present address: Laboratoire de Physique Statistique, Ecole Normale Supérieure, Unité Mixte de Recherche 8550 associée au Centre National de la recherche Scientifique et aux Universités Paris VI et VII, 24 Rue Lhomond, Paris 75231, France.

1742-5468/09/P02060+28$30.00

Contents

1. Introduction

Single-molecule force measuring techniques have made possible the controlled manipulation of individual molecules by applying forces on the piconewton scale. Current force measuring devices include the atomic force microscope, optical and magnetic tweezers, and even microneedles and biological membranes used as force probes. Single-molecule manipulation has been used to investigate many problems in molecular and cellular biophysics (see [1, 2] for recent reviews). To cite just a few examples: the mechanical properties of biopolymers such as DNA [3]–[5] have been established for the first time; the folding/unfolding processes in individual RNA or protein molecules [6]–[8] have been investigated; the interactions between DNA and proteins [9], but also between DNA and RNA, have been studied at the molecular level [10]; the motion of single-molecular motors has also been followed in real time [11]–[15].

An important aspect of single-molecule force experiments is the possibility of monitoring the time evolution of individual molecules by recording the molecular extension. Measuring forces and extensions as functions of time provides a lot of information about thermodynamics and kinetics of individual molecules. A very useful

doi:10.1088/1742-5468/2009/02/P02060

J. Stat. Mech. (2009) P02060

technique for achieving this goal is using optical tweezers, which are suited to accurately measuring forces in the range 0.1–100 pN. Using optical tweezers, it is possible to derive the free energies of formation of biomolecules with good accuracy. At the same time, optical tweezers allow us to investigate questions related to the kinetics of folding, a challenging problem in biophysics and statistical mechanics. A physical entity useful for characterizing the behaviour of complex systems is the free energy landscape. The free energy landscape describes the energetics of the configurational space of a system. Introduced and applied in the context of disordered and glassy systems, this concept finds a major application in small systems, where thermal fluctuations entail large conformational fluctuations and the system can explore a large portion of the configurational space.

In this paper we investigate the thermodynamics and kinetics of force induced folding/unfolding (hereafter referred to as F/U) of short DNA hairpins. Investigating force kinetics of DNA hairpins presents several advantages [16, 17] over other molecular constructs. In particular, DNA sequences can be synthesized with relative ease and DNA degrades less than other molecules (e.g. RNA) do. We carry out single-DNA pulling experiments using optical tweezers to extract information from thermodynamics and kinetics under the application of an external force. The results are compared with theoretical predictions based on the concept of the free energy landscape. The paper is divided up as follows. After giving a brief summary of the type of experiments in section 2, we elaborate on the concept of a free energy landscape applied to nucleic acid hairpins (DNA or RNA) in section 3. Section 4 explains how to extract information about thermodynamics and kinetics from pulling data. An analysis of the kinetic parameters extracted from our experiments is presented in section 5. Section 6 shows an alternative method for deriving free energy differences using fluctuation relations. Finally, in section 7 we discuss how to extract the free energy of formation of the hairpin at zero force, both from kinetics and from fluctuation relations. After section 8, three appendices supplement the results of this paper detailing some technical subjects.

2. Mechanical unfolding of DNA hairpins

Our experimental set-up is shown in figure 1(a). The DNA hairpin is tethered between two beads by using double-stranded DNA (dsDNA) handles. Experiments are carried out in a newly designed miniaturized dual-beam laser optical tweezers apparatus [18]. One bead is immobilized in the tip of a micropipette that is integral to the fluidics chamber; the other bead is captured in an optical trap generated by two counterpropagating laser beams [19]. The force acting on the bead can be directly measured from the change in light momentum deflected by the bead. A steerable optical trap can be moved up and down along the vertical axis so as to repeatedly unfold/refold the molecule. Every pulling cycle consists of a stretching process (hereafter referred to as S) and a releasing (hereafter referred to as R) process. In the stretching part of the cycle the molecule is stretched from a minimum value of the force ($f_{\rm min} \sim 10$ pN), so small that the hairpin is always folded, up to a maximum value of the force ($f_{\rm max} \sim 20$ pN), so large that the hairpin is always unfolded. During the releasing part of the cycle the force is decreased from $f_{\rm max}$ back to $f_{\rm min}$. The force is varied at the same *loading rate* (the rate at which the force is increased

doi:10.1088/1742-5468/2009/02/P02060

J. Stat. Mech. (2009) P02060

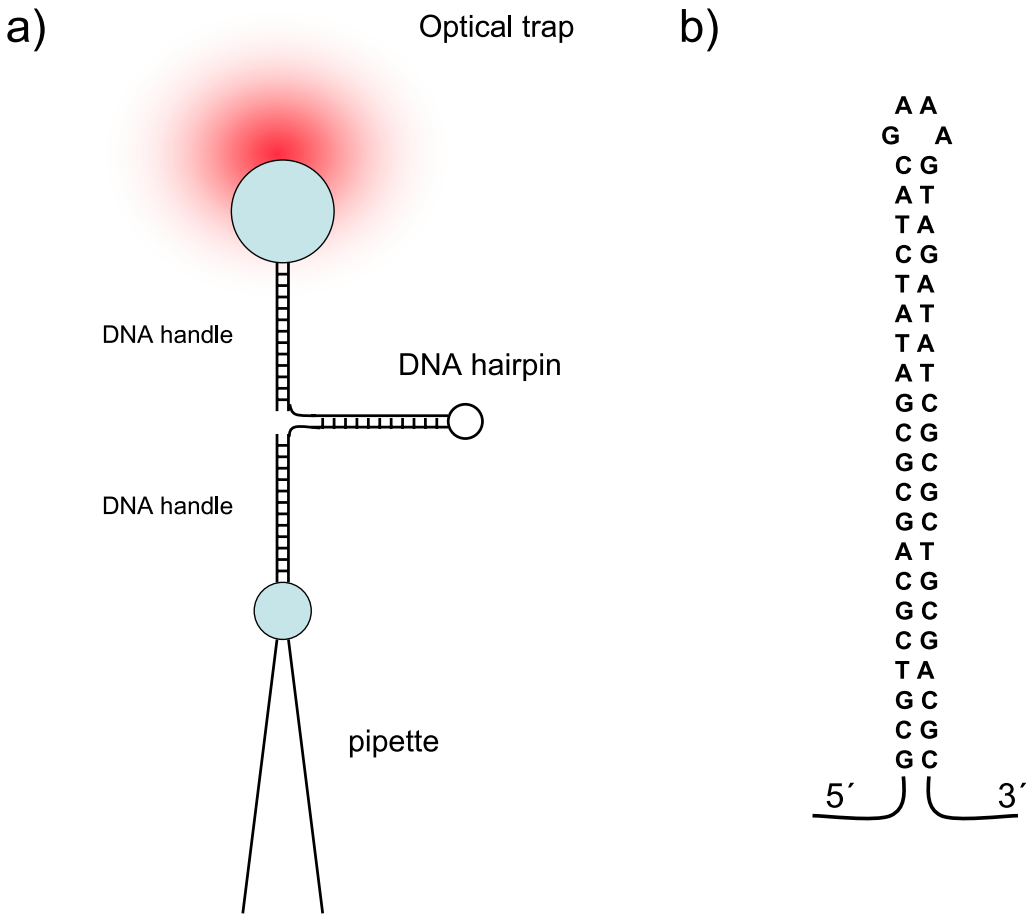

Figure 1. (a) Experimental set-up. (b) DNA hairpin sequence. The 5′ and 3′ labels indicate the polarity of the phosphate chain of the hairpin.

or decreased) in both stretching and releasing stages of the cycle[4], and recorded with an acquisition frequency of 1 kHz. All experiments were done at a temperature 23–24 °C in a 1 M NaCl aqueous buffer with neutral pH (7.5) stabilized with Tris HCl and 1 M EDTA.

The molecular construct is shown in figure 1(b) and consists of a DNA hairpin of 21 base pairs (bps) ending with a tetraloop GAAA. The hairpin is inserted between two identical short dsDNA handles of 29 bps each. The sequence of this DNA hairpin is canonical (i.e. all base pairs are complementary) and has been specifically designed to produce a two-state folder (see below in section 3).

Force–distance curves (FDCs) in our experiments represent the force acting on the molecule as a function of the relative position of the trap along the force axis. From the FDC it is possible to extract the molecular extension, so as to represent the force versus the molecular extension in what is known as a force–extension curve (FEC). Many works

[4] This process is performed at constant pulling speed v. Since the elasticity of DNA (dsDNA handles and unfolded DNA hairpin) is force dependent, strictly speaking the loading/unloading rate r is not constant throughout the pulling process. Nevertheless, in the force range of our experiment the rigidity of the optical trap k_{b} is much smaller than the stiffness of the handles and the unfolded DNA hairpin. Therefore, the effective rigidity (31) is $k_{\mathrm{eff}} \approx k_{\mathrm{b}}$, and our system verifies $r = vk_{\mathrm{eff}} \approx vk_{\mathrm{b}}$.

in single-molecule manipulation often use such representation. However, in many respects it is better to use the trap position rather than the molecular extension to draw pulling curves. In fact, the former is the only parameter that is externally controlled (referred to as the *control parameter* [20]) whereas the latter is subject to fluctuations that introduce additional (albeit small) corrections (e.g. in the measure of the mechanical work exerted upon the molecule). Although both descriptions contain the same information, we will stick to the FDC picture throughout this paper.

Figure 5(a) shows some typical FDCs for the sequence under study at three different loading rates (slow and fast). The FDC shows a linear dependence of the force versus distance as a consequence of our choice of short handles. In fact, because the handles are very rigid (when compared to the rigidity of the trap) the effective rigidity of the system made of bead and handles is mostly determined by the constant rigidity of the Hookean (i.e. linear) optical trap. Force rips are generated each time the molecule folds/unfolds: after unfolding, a segment of 46 nucleotides of ssDNA is released, so the force suddenly drops as the trapped bead relaxes toward the centre of the optical trap; whereas after refolding the closure of the DNA hairpin pulls the bead away from the trap and the force increases.

When pulling at slow loading rates the molecule shows low hysteresis in the value of the unfolding/refolding force. Moreover, the hairpin can execute several F/U transitions during the stretching and releasing stages of the cycle. In contrast, when pulling at fast loading rates, the molecule shows larger hysteresis in the value of the unfolding/refolding force, and multiple F/U transitions are unlikely. The number of transitions observed and how irreversible the stretching and releasing processes are depend on how large the pulling rate r is compared to the typical folding/unfolding rate [48].

3. The free energy landscape

Following the dynamics of the folding/unfolding process in configuration space is a formidable task, due to the large number of interacting degrees of freedom. However, the collective behaviour displayed by the F/U transition suggests a simplified approach: one can judiciously choose one collective *reaction coordinate* and project the many-dimensional energy landscape (where we represent the energy of each microscopic configuration) onto a one-dimensional *free energy* profile, where each point stands for an ensemble of configurations. One minimum of the free energy profile represents the energetically favoured folded state, another one the entropically favoured unfolded state. In between, we find information about how much energy is needed (in the form of either heat or work) to explore intermediate states of the system. In this section we will focus on the case where pressure and temperature are constant, and the applied force is the control parameter, while other variables such as the molecular extension or the position of the trap fluctuate. The effect of the experimental set-up on the free energy landscape is discussed in appendices A and C.

As reaction coordinate, we choose the number of open base pairs n. If N is the number of base pairs in the stem of the hairpin, and L is the number of bases in the loop (and thus the total number of bases in the hairpin is $2N + L$), the configuration with $n = 0$ is the folded state, while the configuration with $n = N$ is the completely unfolded state. In the absence of an externally applied force, we will use the symbol

$G^0(n)$ to denote the free energy to be delivered to the molecule (in the form of heat) in order to break the first n base pairs. $G^0(n)$ can be measured in bulk experiments, e.g. by calorimetry or UV absorbance: by melting oligonucleotides of different lengths we can enforce the desired number n of dissociated base pairs. The free energies of dissociation of the different nearest neighbour base pairs [21], and other different secondary structural elements (e.g. base pair mismatches, loops, etc) are used by Mfold [23] to extract the free energy of formation of the DNA molecule. In general, $G^0(n)$ will be a monotonically increasing function of n whenever base pairs dissociate; however, it may decrease in the presence of entropic structural elements such as loops [22].

3.1. The effect of force

What is the effect of an externally applied force f on the free energy landscape $G^0(n)$? To answer this question, we introduce the force dependent free energy landscape $G(x_n, f)$, where x_n is the distance between the $3'$ and the $5'$ extremities of the hairpin, measured along the direction of the applied force [24, 25]. We find it convenient to express the free energy in terms of x_n because this quantity, unlike n, is experimentally accessible.

In the folded $n = 0$ state, in the presence of an external force $f \neq 0$, the hairpin is always oriented along the force axis; therefore x_0 is equal to the diameter of the hairpin d_0 (typically about 2 nm). If $f = 0$, then the hairpin is generally not aligned, and all we can say is that $x_0 \leq d_0$. For any intermediate state with $0 < n < N$, x_n is equal to d_0, plus the equilibrium extension $x^{l_n}(f)$ of a ssDNA molecule with contour length $l_n = 2nd$ (this relation can change in the presence of structural motifs such as base pair mismatches) if d is the interbase distance. The length $x^{l_n}(f)$ is found by inverting the thermodynamic force–extension curve

$$f = F^{l_n}_{\mathrm{ssDNA}}(x). \tag{1}$$

The explicit form of (1) depends on the particular model assumed (the most popular being the freely jointed chain and the worm-like chain). In the totally unfolded state with $n = N$, x_N is the equilibrium extension $x^{l_N}(f)$ of a ssDNA molecule with contour length $l_N = (2N + L)d$. In summary,

$$x_n(f) = (1 - \delta_{n,N})d_0 + x^{l_n}(f), \qquad l_n = 2nd + \delta_{n,N}Ld. \tag{2}$$

Note that in (1) we assume thermodynamic equilibrium for the ssDNA. It would be possible to include elastic free energy fluctuations in the stretching part of the free energy corresponding to the ssDNA to substitute the discrete x_n with a continuous variable x, but this would not change the predictions of the model much.

In the presence of an external force the free energy landscape $G(x_n, f)$ is tilted along the reaction coordinate:

$$G(x_n, f) = G^0(n) + G_{\mathrm{ssDNA}}(0 \to x^{l_n}; f) - f x_n, \tag{3}$$

where we have introduced

$$G_{\mathrm{ssDNA}}(0 \to x^{l_n}; f) = \int_0^{x^{l_n}} F^{l_n}_{\mathrm{ssDNA}}(y)\,\mathrm{d}y, \tag{4}$$

that is the reversible work needed to stretch a segment of ssDNA of contour length l_n from an initial extension equal to 0 to a final extension $x^{l_n}(f)$ (see figure 2(a)), or, in other words, the area under the force–extension curve (1) between 0 and x^{l_n}.

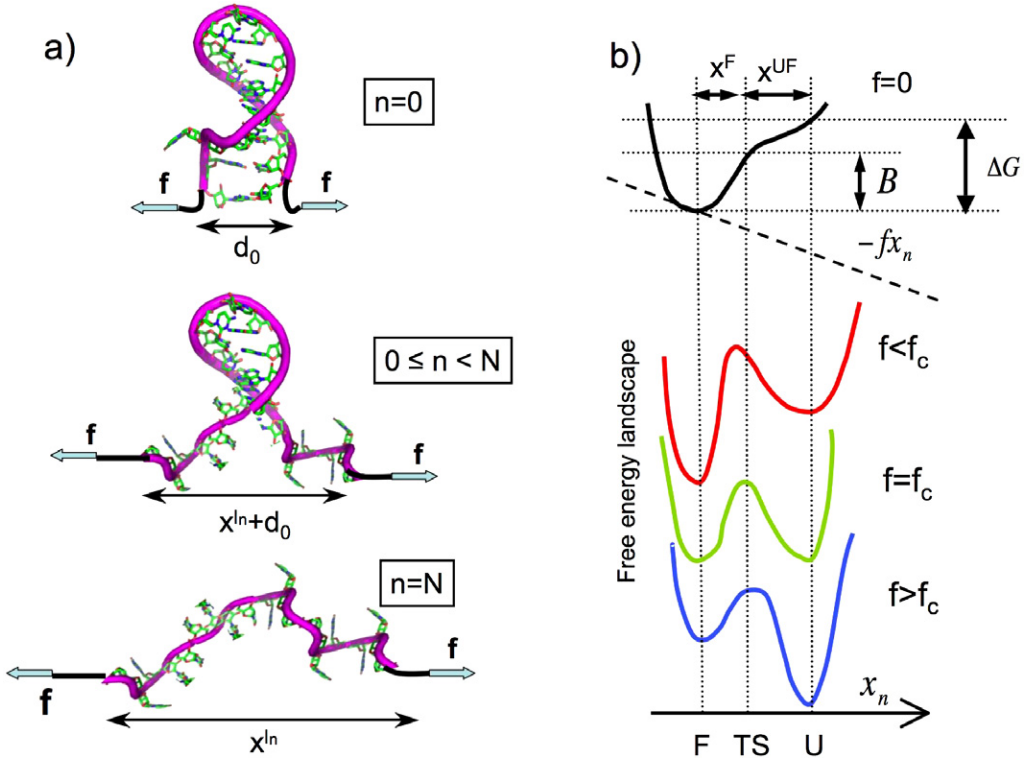

Figure 2. (a) Schematic picture of the different configurations of a hairpin with N base pairs at force f. For all configurations where the molecule is not completely unfolded, the molecular extension is equal to $x^{l_n}+d_0$ where x^{l_n} is the extension at force f of the released $2n$ bases of ssDNA. (b) Schematic picture of the free energy landscape at different forces f. The most important parameters are the distances from the transition state (TS) to the folded (F) and unfolded (U) states: x^{F} and x^{UF}, respectively; the free energy difference $\Delta G(f)$ and the barrier $B(f)$. As force increases the free energy landscape is tilted down, favouring configurations of large extension x_n.

Using (4), after a change of integration variable, we can rewrite the free energy landscape (3) as

$$G(x_n, f) = G^0(n) - \int_0^f x_n(f')\,\mathrm{d}f' + \delta_{n,N} f d_0. \tag{5}$$

From the free energy landscape (3) we can define two important force dependent parameters. The first is the free energy difference between the folded and the unfolded states,

$$\Delta G(f) = G(x_N, f) - G(x_0, f) = \Delta G_0 + G_{\mathrm{ssDNA}}(0 \to x^{l_N}; f) - (x^{l_N} - d_0)f, \tag{6}$$

where $\Delta G_0 = \Delta G(f=0) = G^0(N) - G^0(0)$ denotes the free energy of formation of the hairpin at zero force. In what follows we will simplify the notation by defining

$$x_{\mathrm{m}}(f) = x^{l_N}(f) - d_0. \tag{7}$$

$x_{\rm m}$ depends on the force f and is equal to the released molecular extension when the hairpin unzips completely. In this notation we have

$$\Delta G(f) = G(x_N, f) - G(x_0, f) = \Delta G_0 + G_{\rm ssDNA}(0 \to x^{l_N}; f) - f x_{\rm m}. \tag{8}$$

The other important parameter is the free energy barrier, equal to the free energy difference between the transition and the folded states,

$$B(f) = G(x^{\rm F}, f) - G(x_0, f) = B_0 + G_{\rm ssDNA}(0 \to x^{l_{\rm F}}; f) - f x^{\rm F}, \tag{9}$$

where $x^{\rm F}$ is defined as the value of x_n where $G(x_n, f)$ is maximum, $B_0 = G^0(n^{\rm F}) - G^0(0)$ is the free energy barrier at zero force, $n^{\rm F}$ is the number of base pairs released at the transition state at force f, and $l_{\rm F} \equiv l_{n^{\rm F}}$.

We stress that the parameters $\Delta G(f)$ and $B(f)$, as determined from the shape of the free energy landscape $G(x_n, f)$, depend directly on the applied force. Moreover, the relevant distances $x_{\rm m}$ and $x^{\rm F}$ are also expected to depend on the force due to the dependence of the molecular extension of the ssDNA on force, as shown in (1). Yet, such dependence is expected to be very small for forces in the vicinity of the F/U transition (see below). In what follows, and in order to lighten the notation, we will not indicate explicitly such force dependence for these distances. For later use we define the following quantities:

$$\Delta G_1(f) = \Delta G_0 + G_{\rm ssDNA}(0 \to x^{l_N}; f) \Longrightarrow \Delta G(f) = \Delta G_1(f) - f x_{\rm m}, \tag{10}$$

$$B_1(f) = B_0 + G_{\rm ssDNA}(0 \to x^{l_{\rm F}}; f) \Longrightarrow B(f) = B_1(f) - f x^{\rm F}. \tag{11}$$

As we will see below, ΔG_1, $x_{\rm m}$ and $x^{\rm F}$ can be directly measured in pulling experiments.

In the previous computation, we have neglected the work needed to orient the hairpin along the force axis. On treating the elastic response of the folded hairpin as a polymer of contour length equal to the hairpin diameter d_0 and persistence length P, the work necessary to orient the hairpin along the force axis is inversely proportional to P. For a rigid object P is large, so the free energy of orienting the hairpin is indeed expected to be negligible. Not so the effect of the hairpin diameter, as shown in (5).

3.2. Kramers–Bell kinetic rates

According to the Kramers–Bell theory [26], the kinetic rates of unfolding and folding under tension in a two-state folder are given by

$$k_{\rightarrow}(f) = k_0 \exp\left[-\left(\frac{G(x^{\rm F}, f)}{k_{\rm B}T}\right)\right], \tag{12a}$$

$$k_{\leftarrow}(f) = k_0 \exp\left[-\left(\frac{-G(x_N, f) + G(x_0, f) + G(x^{\rm F}, f)}{k_{\rm B}T}\right)\right]. \tag{12b}$$

$k_{\rightarrow}(f)$ ($k_{\leftarrow}(f)$) describes the kinetic rate for jumping over the transition state from the folded (unfolded) state. k_0 stands for the attempt frequency of the hairpin (which may get contributions from the instrument and the whole molecular construct), $k_{\rm B}$ and T being respectively the Boltzmann constant and the temperature of the bath. The rates (12a)

and (12*b*) satisfy detailed balance,

$$\frac{k_{\rightarrow}(f)}{k_{\leftarrow}(f)} = \exp\left(-\frac{G(x_N,f)-G(x_0,f)}{k_{\mathrm{B}}T}\right) = \exp\left(-\frac{\Delta G_0 + G_{\mathrm{ssDNA}}(0\rightarrow x^{l_N};f) - fx_{\mathrm{m}}}{k_{\mathrm{B}}T}\right) = \exp\left(-\frac{\Delta G(f)}{k_{\mathrm{B}}T}\right), \tag{13}$$

where $\Delta G(f)$ has been defined in (8). The coexistence force f_{c} is defined as the value of the force at which the equilibrium constant is equal to 1,

$$k_{\mathrm{c}} = k_{\rightarrow}(f_{\mathrm{c}}) = k_{\leftarrow}(f_{\mathrm{c}}), \tag{14}$$

k_{c} being the coexistence rate. According to (13), this corresponds to $\Delta G(f_{\mathrm{c}}) = 0$, or

$$\Delta G_1(f_{\mathrm{c}}) = \Delta G_0 + G_{\mathrm{ssDNA}}(0\rightarrow x^{l_N};f_{\mathrm{c}}) = f_{\mathrm{c}}x_{\mathrm{m}}. \tag{15}$$

Summarizing, the kinetic rates (12*a*) and (12*b*) can be rewritten in a more compact form,

$$k_{\rightarrow}(f) = k_0 \exp\left[-\left(\frac{B_1(f)-fx^{\mathrm{F}}}{k_{\mathrm{B}}T}\right)\right], \tag{16a}$$

$$k_{\leftarrow}(f) = k_0 \exp\left[-\left(\frac{B_1(f)-\Delta G_1(f)+fx^{\mathrm{UF}}}{k_{\mathrm{B}}T}\right)\right], \tag{16b}$$

where

$$x_{\mathrm{m}} = x^{\mathrm{F}} + x^{\mathrm{UF}} \tag{17}$$

is equal to the change in molecular extension across the F/U transition. The terms $\Delta G_1(f), B_1(f)$ are given in (10) and (11), while each stretching contribution (contained in those terms) of the type $G_{\mathrm{ssDNA}}(0\rightarrow x^{l}(f))$ has been defined in (4) and (1).

3.3. Simplified version of the rates

In a further simplified description [27], it is common to neglect any force dependence for $\Delta G_1(f)$ and $B_1(f)$ in (16*a*) and (16*b*), so as to incorporate these quantities into effective values for the barrier B_1 and the free energy difference ΔG_1 measured at the transition force f_{c}. This means that $\Delta G_1(f) \simeq \Delta G_1(f_{\mathrm{c}})$ and $B_1(f) \simeq B_1(f_{\mathrm{c}})$ if f is not too far from f_{c}. This approximation is justified because the elastic contributions contained in those terms vary much less with force than the products $fx^{\mathrm{F}}, fx^{\mathrm{UF}}$ do. A mathematical proof of this result is shown in appendix B. In what follows we will drop any force dependence in the effective parameters B_1 and ΔG_1 and write the kinetic rates as follows:

$$k_{\rightarrow}(f) = k_{\mathrm{m}} \exp\left(\frac{fx^{\mathrm{F}}}{k_{\mathrm{B}}T}\right), \qquad k_{\leftarrow}(f) = k_{\mathrm{m}} \exp\left(\frac{\Delta G_1 - fx^{\mathrm{UF}}}{k_{\mathrm{B}}T}\right), \tag{18}$$

where k_{m} corresponds to the unfolding rate at zero force and is given by

$$k_{\mathrm{m}} = k_0 \exp\left(-\frac{B_1}{k_{\mathrm{B}}T}\right). \tag{19}$$

J. Stat. Mech. (2009) P02060

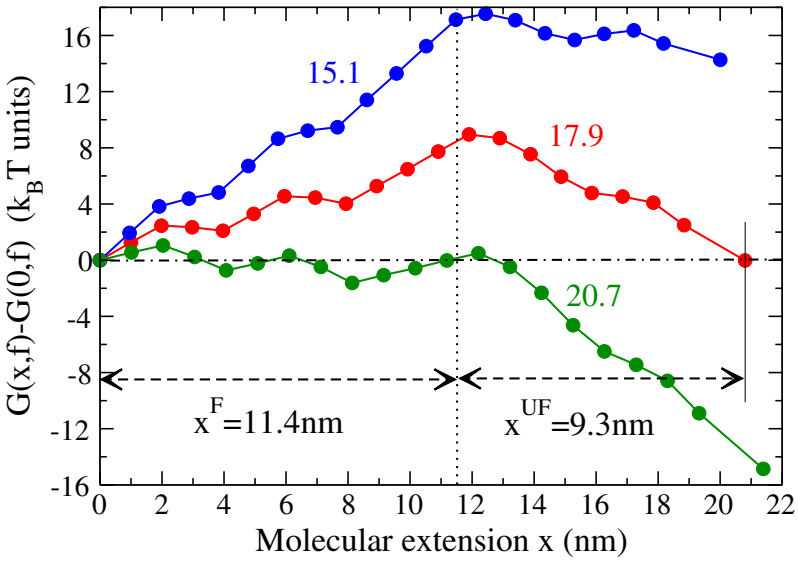

Figure 3. Free energy landscape at various forces for the hairpin sequence shown in figure 1(b). The stretching contribution has been calculated from Mfold using (40) and (41) (see below in section 7). Moreover, the effect of the diameter d_0 has been included in the calculation. The values shown for the distances $x^{\mathrm{F}}, x^{\mathrm{UF}}$ are approximately 1 nm larger than the values found in our experiments. However, the value for the fragility μ (20) inferred from these distances (0.1) is compatible with that found in the experiments (0.0975; see table 1).

As we will see in section 4, the simplified rates (18) reproduce the experimental results reasonably well.

The success of the two-state model in reproducing the kinetics of the force induced F/U reactions depends on the hairpin sequence. In the absence of structural motifs that may induce alternative F/U pathways or intermediate states (see for example [28]), a short hairpin (a few tens of base pairs) will display cooperative two-state behaviour. In addition, if the sequence is designed in such a way that the free energy landscape along the reaction coordinate has a single barrier, then such a molecule is expected to behave as a two-state folder displaying simple Arrhenius kinetics. In this work we have designed a DNA sequence (see figure 1(b)) that has such properties. The free energy landscape as a function of the molecular extension has been calculated at various forces using the free energy values from Mfold and the elastic properties of ssDNA. In figure 3 we show the calculated free energy landscape at various forces around the coexistence force $f_{\mathrm{c}} \simeq 17.9$ pN, where the free energies of the folded and unfolded states are equal.

3.4. The fragility

An important aspect of the Kramers–Bell rates (18) is their strong dependence on force which is determined by the values of x^{F} and x^{UF}. If $x^{\mathrm{F}} \gg x^{\mathrm{UF}}$, then the transition state is located far away from the folded state and the molecule deforms considerably before it unfolds. In the other case, when $x^{\mathrm{UF}} \gg x^{\mathrm{F}}$, the transition state is located close to the folded state and the molecule unfolds without deforming much. A quantitative measure

of how much the native structure deforms before unfolding occurs is given by the fragility parameter [29]–[32]

$$\mu = \frac{x^{\mathrm{F}} - x^{\mathrm{UF}}}{x^{\mathrm{F}} + x^{\mathrm{UF}}} = \frac{x^{\mathrm{F}} - x^{\mathrm{UF}}}{x_{\mathrm{m}}}. \tag{20}$$

μ lies in the range $[-1:1]$ and defines the degree of compliance of the molecule under the effect of tension. Fragile or compliant molecules are those in which x^{F} is larger than x^{UF} and μ is positive. In contrast, when x^{UF} is larger than x^{F} and μ is negative, we talk about brittle structures. The fragility has been proved to be a useful parameter for describing the mechanical unfolding of RNA hairpins with more than one transition state [32].

4. Breakage force kinetics

In order to manipulate a DNA hairpin using optical tweezers, the free ends of the molecule are attached to micron-sized beads by using dsDNA handles. In this experimental configuration (see figure 1(a)), the force fluctuates and the control parameter is the extension between the centre of the trap and the tip of the micropipette. This experimental set-up corresponds to the so called mixed ensemble. It is then possible to describe the F/U kinetics of the DNA hairpin using the two-state model depicted in figure 2, taking into account that the variable that controls the shape of the free energy landscape is the trap–pipette distance rather than the force. The mixed ensemble gets contributions from the different elements of the experimental set-up. In their simplified form the kinetic rates in the mixed ensemble can be shown to obey (18) with identical force dependent terms in the exponent (i.e. equal values for $\Delta G_1, x^{\mathrm{F}}, x^{\mathrm{UF}}$) but different prefactors (see appendix C in [33]).

The simplest way to extract the values of $\Delta G_1, x^{\mathrm{F}}, x^{\mathrm{UF}}$ from the pulling data is to analyse the distribution of first-rupture forces during stretching and releasing parts of the cycle, f^*_{S} and f^*_{R}. The first-rupture force $f^*_{\mathrm{S\,(R)}}$ during the stretching (releasing) part of the cycle is the value of the force at which the first force rip is observed at the time where the first jump occurs. An illustration is shown in figure 4. Useful quantities that can be measured in pulling experiments are: the survival probability $P_{\mathrm{S\,(R)}}(f)$ that the molecule remains in the folded (unfolded) state during the stretching (releasing) process until reaching the force f, the mean value and the variance of the first-rupture forces $f^*_{\mathrm{S\,(R)}}$.

Survival probability. The distribution $P_{\mathrm{S\,(R)}}(f)$ satisfies the following master equation:

$$\frac{\mathrm{d}P_{\mathrm{S\,(R)}}(f(t))}{\mathrm{d}t} = -k_{\rightarrow(\leftarrow)}(f(t))P_{\mathrm{S\,(R)}}(f(t)). \tag{21}$$

$P_{\mathrm{S\,(R)}}(f)$ is related to the experimentally measured distribution of first-rupture forces, $\rho_{\mathrm{S\,(R)}}(f)$, by

$$P_{\mathrm{S}}(f) = 1 - \int_{f_{\min}}^{f} \rho_{\mathrm{S}}(f')\,\mathrm{d}f', \qquad P_{\mathrm{R}}(f) = 1 - \int_{f}^{f_{\max}} \rho_{\mathrm{R}}(f')\,\mathrm{d}f', \tag{22}$$

J. Stat. Mech. (2009) P02060

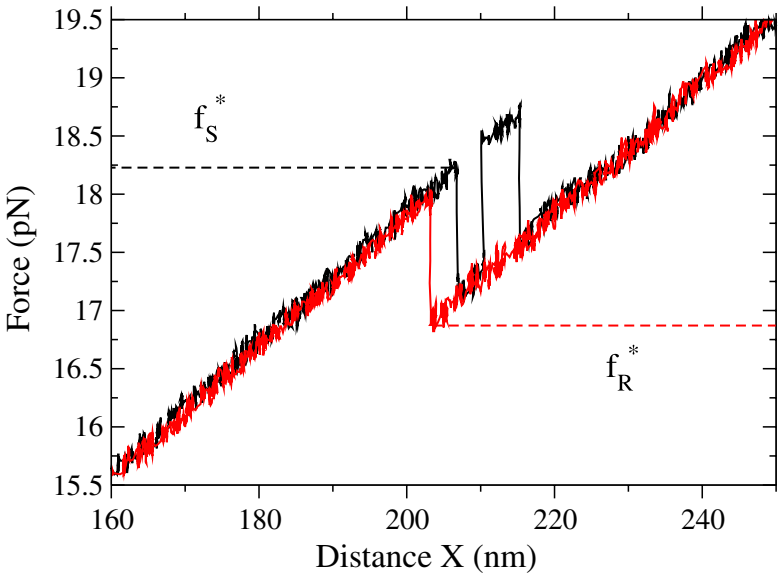

Figure 4. A representative FDC showing the stretching (black) and releasing (red) parts of a pulling cycle. It shows the first-rupture force during stretching ($f_{\rm S}^*$) and releasing ($f_{\rm R}^*$) processes.

where $f_{\rm min}$ ($f_{\rm max}$) is the initial (final) force during the stretching–releasing cycles. For a protocol at a constant loading/unloading rate r, $P_{\rm S\,(R)}(f)$ can be exactly computed:

$$P_{\rm S}(f) = \exp\left[-\left(\frac{k_{\rm B}T}{rx^{\rm F}}\left(k_{\rightarrow}(f) - k_{\rightarrow}(f_{\rm min})\right)\right)\right], \tag{23a}$$

$$P_{\rm R}(f) = \exp\left[-\left(\frac{k_{\rm B}T}{rx^{\rm UF}}\left(k_{\leftarrow}(f) - k_{\leftarrow}(f_{\rm max})\right)\right)\right], \tag{23b}$$

where we used the unfolding (folding) rates given in (18) [34]. In the limit $f_{\rm min} \ll f_{\rm c}$ (S process) and $f_{\rm max} \ll f_{\rm c}$ (R process), the function $\log[-r(\log(P_{\rm S\,(R)}(f)))]$ is given by

$$\log[-r(\log(P_{\rm S}(f)))] = \log\left(\frac{k_{\rm B}Tk_{\rm m}}{x^{\rm F}}\right) + \left(\frac{x^{\rm F}}{k_{\rm B}T}\right) f, \tag{24a}$$

$$\log[-r(\log(P_{\rm R}(f)))] = \log\left(\frac{k_{\rm B}Tk_{\rm m}}{x^{\rm UF}}\right) + \frac{\Delta G_1}{k_{\rm B}T} - \left(\frac{x^{\rm UF}}{k_{\rm B}T}\right) f. \tag{24b}$$

These results show that the function $\log[-r(\log(P_{\rm S\,(R)}(f)))]$, plotted as a function of the applied force f, is a straight line with a slope inversely proportional to the position of the kinetic barrier $x^{\rm F}$ ($x^{\rm UF}$) and intercepts $(a_{\rm S}, a_{\rm R})$ related to the rate $k_{\rm m}$ and the free energy difference ΔG_1 [34]. To extract the value of ΔG_1, we do linear fits to (24*a*) and (24*b*), and then use the independent coefficients $a_{\rm S}, a_{\rm R}$ to obtain

$$\frac{\Delta G_1}{k_{\rm B}T} = a_{\rm R} - a_{\rm S} + \log\left(\frac{x^{\rm UF}}{x^{\rm F}}\right). \tag{25}$$

In order to extract B_1 we can use the relation (19), $B_1 = -k_{\rm B}T\log(k_{\rm m}/k_0)$ where $k_{\rm m}$ can be extracted from the value of $a_{\rm S}$ but k_0 is unknown. In order to determine B_1 one needs

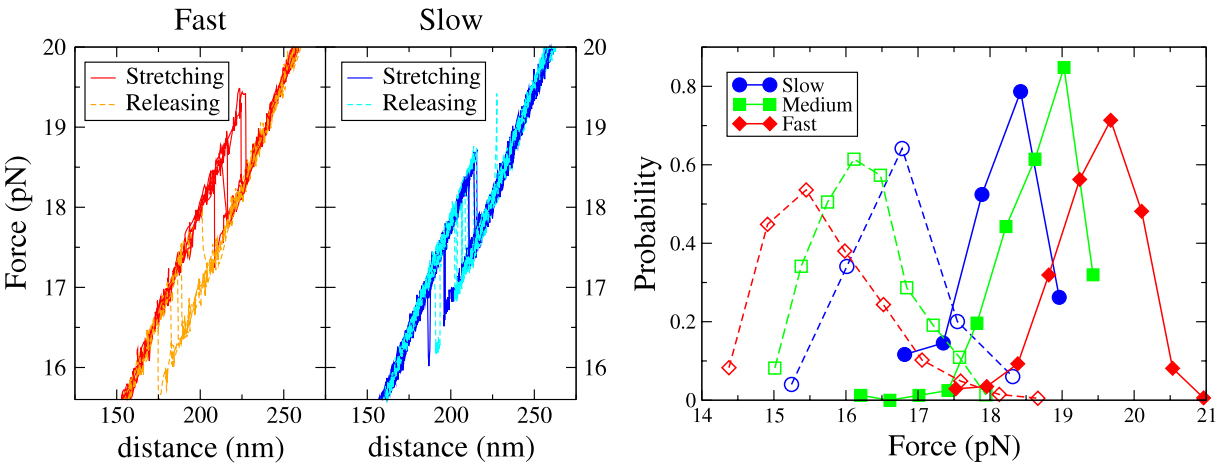

Figure 5. (a) Force–distance curves (FDCs) corresponding to five cycles at fast and slow pulling speeds (200 nm s^{-1} and 25 nm s^{-1} respectively, corresponding to loading rates of 8.1 and 1.0 pN s^{-1}). Continuous red (dashed orange) lines correspond to fast stretching (releasing) parts of the cycle. Continuous blue (dashed cyan) lines correspond to slow stretching (releasing) parts of the cycle. Note that hysteresis increases with the pulling speed. Moreover, FDCs at slow speeds show several transitions between the folded and the unfolded states. (b) First-rupture force distributions for the stretching (continuous lines) and releasing process (dashed lines) for three molecules at three different loading rates $r = 1.76$ pN s^{-1} (blue), $r = 4.8$ pN s^{-1} (green), $r = 14.5$ pN s^{-1} (red).

to make further assumptions. For example, it is possible to use effective one-dimensional Kramers models applied to molecular free energy landscapes [32, 35, 36] to infer the value of B_1. Figure 6 shows an experimental test of (24*a*), (24*b*) using the results shown in figure 5(b).

Mean and variance of first-rupture forces. The dependence on the rate r of the mean value and the standard deviations of $f_{\rm S}^*$ and $f_{\rm R}^*$ can be computed in the relevant experimental regime, that is when

$$a \equiv \frac{k_{\rightarrow(\leftarrow)}(f_{\rm c})k_{\rm B}T}{rx^{\rm F(UF)}} \ll 1, \tag{26}$$

($f_{\rm c}$ being the coexistence force) [37]. The result is

$$\langle f_{\rm S}^* \rangle = \frac{k_{\rm B}T}{x^{\rm F}}[C + \log(r)] + {\rm O}(a), \qquad \langle \sigma_{f_{\rm S}^*} \rangle = \frac{k_{\rm B}T}{x^{\rm F}} + {\rm O}(a), \tag{27}$$

$$\langle f_{\rm R}^* \rangle = \frac{k_{\rm B}T}{x^{\rm UF}}[C' - \log(r)] + {\rm O}(a), \qquad \langle \sigma_{f_{\rm R}^*} \rangle = \frac{k_{\rm B}T}{x^{\rm UF}} + {\rm O}(a), \tag{28}$$

where $\langle \sigma_{f_{\rm S}^*} \rangle, \langle \sigma_{f_{\rm R}^*} \rangle$ denote the rms deviation of the first-rupture forces. The constants C and C' depend on the characteristics of the molecule and on the initial force values during the stretching and releasing processes respectively. Equations (24*a*), (24*b*) and (27), (28) provide a way to extract the relevant parameters that characterize the free energy landscape from the experimental data. A test of the validity of (27), (28) is shown in figure 7.

J. Stat. Mech. (2009) P02060

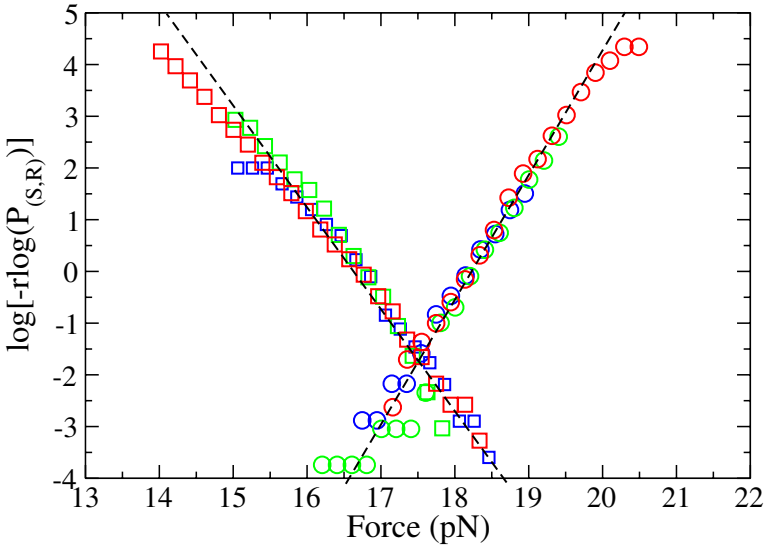

Figure 6. Experimental data for $\log(-r\log(P_{(\mathrm{R,S})}))$ plotted as function of force can be fitted to straight lines according to (24*a*), (24*b*). The slopes of the lines give the distances $x^{\mathrm{F}} = 9.8$ nm, $x^{\mathrm{UF}} = 8.1$ nm (see table 1). Data correspond to three different molecules pulled at different loading rates $r = 1.76$ pN s^{-1} (blue), $r = 4.8$ pN s^{-1} (green), $r = 14.5$ pN s^{-1} (red). Circles correspond to the stretching process. Squares correspond to the releasing process. Note that the value of the force at which folding and unfolding lines cross each other ($\simeq$17.5 pN) lies fairly close to the average coexistence force, 17.75 pN (see table 1).

5. Kinetic parameters for the hairpin

In this section we use the already cited experimental data to extract the parameters that characterize the free energy landscape and the kinetics of the hairpin. A summary of the results obtained by analysing data for 11 molecules pulled at different speeds is shown in table 1. We have extracted the different values of the parameters for each molecule to find the mean and the standard deviation. The values $x^{\mathrm{F}}, x^{\mathrm{UF}}$ have been extracted from the linear fits (24*a*), (24*b*), whereas x_{m} and μ are given by (17), (20). For each molecule the value of ΔG_1 has been obtained from (25) whereas the coexistence force f_{c} and the coexistence rate k_{c} are extracted from (15), (14) and (18):

$$f_{\mathrm{c}} = \frac{\Delta G_1}{x_{\mathrm{m}}}, \qquad k_{\mathrm{c}} = k_{\mathrm{m}} \exp\left(\frac{f_{\mathrm{c}} x^{\mathrm{F}}}{k_{\mathrm{B}} T}\right). \tag{29}$$

To complement such estimates we also show another estimate ($\bar{f}_{\mathrm{c}}$) for the average coexistence force which corresponds to the average first-rupture forces during the stretching and release parts of the cycle:

$$\bar{f}_{\mathrm{c}} = \tfrac{1}{2}(\overline{f^*_{\mathrm{S}}} + \overline{f^*_{\mathrm{R}}}). \tag{30}$$

In addition, we also verify that the product of the coexistence force $\bar{f}_{\mathrm{c}}$ (30) times the extension x_{m} averaged over all molecules is compatible with the average value of ΔG_1. Finally, we also show three more quantities: (1) the average force jump across the

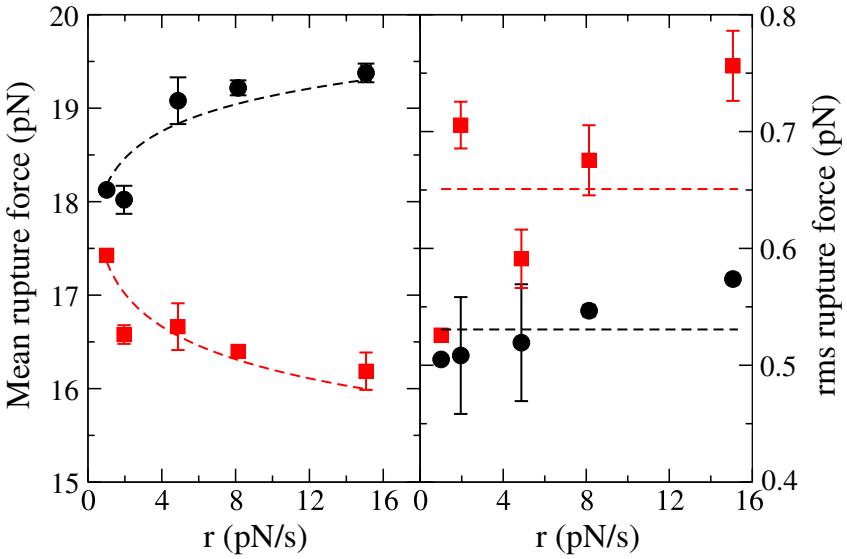

Figure 7. Average and rms deviation of first-rupture forces as a function of the loading rate. Data have been taken by averaging over different molecules at different loading rates (see table 1). The average rupture force (left panel) has been fitted to (27) fixing the values $x^{\mathrm{F}} = 9.8$ nm, $x^{\mathrm{UF}} = 8.1$ nm (table 1). We get $C = 43.64, C' = 34.35$ for the best fit. The rms of the rupture force (right panel) is constant with the loading rate (28) but cannot be fitted to (28) with the values of $x^{\mathrm{F}}, x^{\mathrm{UF}}$ obtained from the survival probability analysis. Instead we get $x^{\mathrm{F}} = 7.74$ nm, $x^{\mathrm{UF}} = 6.34$ nm (again compatible with $\mu = 0.1$), which however are 30% smaller than the expected values.

Table 1. Mean and standard deviations of different parameters obtained from the kinetic experiments. Averages are taken over 11 different molecules that have been pulled at different pulling speeds: 18.5 nm s^{-1} or 1 pN s^{-1} (1 molecule, 193 cycles), 36.5 nm s^{-1} or 1.95 pN s^{-1} (2 molecules, 160 cycles), 86.2 nm s^{-1} or 4.88 pN s^{-1} (3 molecules, 570 cycles), 156 nm s^{-1} or 8.1 pN s^{-1} (2 molecules, 725 cycles), 274.3 nm s^{-1} or 14.9 pN s^{-1} (3 molecules, 1580 cycles).

x^{F} (nm)	x^{UF} (nm)	x_{m} (nm)	μ	f_{c} (pN)	$\bar{f}_{\mathrm{c}}$ (pN)
9.87(36)	8.13(33)	18.06(52)	0.097(23)	17.91(09)	17.75(08)
ΔG_1 ($k_{\mathrm{B}}T$)	$\bar{f}_{\mathrm{c}} \cdot x_{\mathrm{m}}$ ($k_{\mathrm{B}}T$)	k_{c} (Hz)	Δf (pN)	k_{eff} (Hz)	Δx (nm)
78.7(2.4)	78.0(2.3)	0.58(08)	1.230(47)	0.0544(10)	22.6(1.2)

transition, Δf; (2) the average slope of the FDC corresponding to the combined stiffness k_{eff} of bead and handles [38, 39],

$$\frac{1}{k_{\mathrm{eff}}} = \frac{1}{k_{\mathrm{b}}} + \frac{1}{k_{\mathrm{h}}}; \tag{31}$$

and (3) the average retraction of the combined extension of the bead and handles ($x_{\mathrm{b}} + x_{\mathrm{h}}$) induced by the force change, $\Delta x = \Delta f / k_{\mathrm{eff}}$.

Table 2. Mean and standard deviations of free energy parameters obtained from the kinetic measurements. Averages are taken over 11 different molecules that have been pulled at different pulling speeds: 18.5 nm s^{-1} or 1 pN s^{-1} (1 molecule, 193 cycles), 36.5 nm s^{-1} or 1.95 pN s^{-1} (2 molecules, 160 cycles), 86.2 nm s^{-1} or 4.88 pN s^{-1} (3 molecules, 570 cycles), 156 nm s^{-1} or 8.1 pN s^{-1} (2 molecules, 725 cycles), 274.3 nm s^{-1} or 14.9 pN s^{-1} (3 molecules, 1580 cycles).

f_c (pN)	x_{ssDNA} (nm)	d_0 (nm)	$(\Delta G_{ssDNA})^{kin}$ (k_BT)
17.91	23.3	2.0	30.24
$(\Delta G_1)^{kin}$ (k_BT)	$(\Delta G_0)^{kin}$ (k_BT)	$(\Delta G_0)^{kin}$ (kcal mol^{-1})	Mfold (kcal mol^{-1})
78.7(2.4)	57.2(2.4)	33.7(1.5)	36.81

From table 1 there emerges a remarkable fact: the expected molecular extension x_m at $f_c = 17.91$ pN is 3 nm smaller than the change in extension of the combined system formed by bead and handles, which is around 21.30 nm if we subtract from the total extension of the ssDNA (around 23.30 nm; see table 2) the diameter of the hairpin $d_0 = 2$ nm. Is this expected? What is the real average change in molecular extension of the hairpin across the F/U transition? The net change in molecular extension across the transition can be estimated from the average retraction experienced by bead and handles, $\Delta x = \Delta f / k_{eff}$.

Assuming that handles have a large but finite stiffness (around 500 pN μm^{-1}), part of the retraction ($\simeq$10% of the total released molecular extension) might be accounted for by the retraction of the handles. This makes $\Delta x \simeq 22.6$ (table 1) an upper bound to the molecular extension released by the ssDNA.

An important feature of our experiments is the variability observed in the values measured for different molecules. In figure 8 we show histograms of values obtained for a given set of parameters. Although distances x^F, x^{UF}, x_m and the free energy value, ΔG_1, typically show a 15% variation around the average value, other quantities like μ or k_c show a larger variability.

Is it possible to infer the value ΔG_0 from the reported value for ΔG_1? The inclusion of the stretching contributions in order to infer the value of ΔG_0 is discussed below in section 7.

6. Free energy recovery

Alternative methods for extracting the free energy difference ΔG_1 are provided by fluctuation relations. Fluctuation relations are symmetry identities that relate the probability of a system absorbing or releasing a given amount of energy from or to the environment during irreversible processes. In our pulling experiments, single molecules are in a transient nonequilibrium state, as revealed by the systematic hysteresis observed between the stretch and release processes for forces around the coexistence region. When the trap is moved fast enough, then the free energy landscape is modified too quickly and the molecule cannot populate the different states (folded and unfolded) according to the Boltzmann–Gibbs weight. Under equilibrium conditions, (13) predicts

$$\frac{p_{UF}(f)}{p_F(f)} = \frac{k_{\rightarrow}(f)}{k_{\leftarrow}(f)} = \exp\left(-\frac{\Delta G(f)}{k_BT}\right). \tag{32}$$

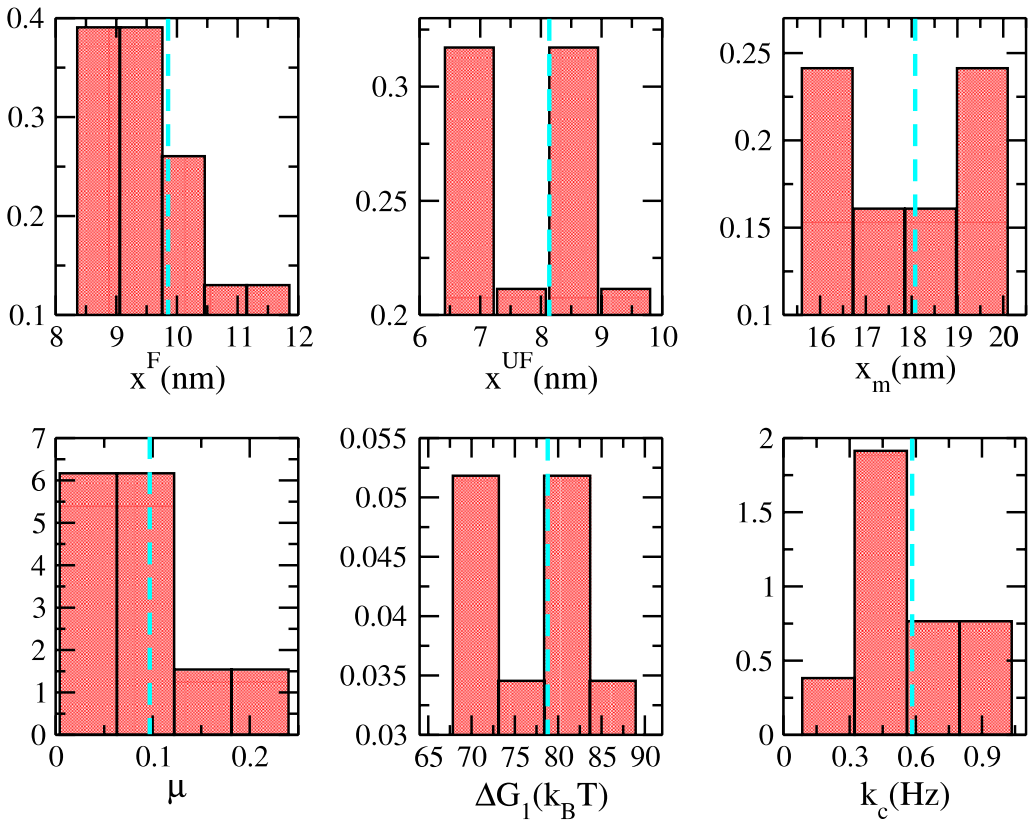

Figure 8. Histograms of some of the parameters reported in table 1. The statistics is collected over 11 molecules pulled at different speeds (see caption of table 1 for more details). The vertical dashed lines (cyan colour) show the mean of the distribution as given in table 1.

Hysteresis effects indicate that measured populations of folded and unfolded molecules $p_{\rm UF}(f), p_{\rm F}(f)$, averaged over many pulling cycles, will not satisfy (32). This precludes the possibility of validity of the thermodynamic equilibrium in our pulling experiments. Note that mechanical equilibrium is probably satisfied at the experimentally accessible pulling speeds, as revealed by the fact that all other relaxational timescales in the system (beads, handles and ssDNA) are much shorter than the F/U timescale [40]–[42].

6.1. The Crooks fluctuation relation

Let $W_{\rm S\,(R)}$ denote the mechanical work exerted on the molecule by moving the optical trap. This is given by

$$W_{\rm S\,(R)} = \int_{X_{\rm min}}^{X_{\rm max}} {\rm d}X F_{\rm S\,(R)}(X), \tag{33}$$

where the subscript S (R) refers to the stretching (releasing) stage of the cycle. In what follows, we will take $W_{\rm S}$ and $W_{\rm R}$ as positive and negative quantities respectively, although, strictly speaking and according to (33), both have positive signs. In fact, during the stretching (releasing) parts of the cycle the optical trap delivers (extracts) mechanical

work to (from) the molecule. During the stretching part of the cycle the work is positive ($\mathrm{d}X > 0$) whereas during the releasing part of the cycle it is negative ($\mathrm{d}X < 0$). By repeatedly pulling the molecule many times we can measure the stretching and releasing work distributions,

$$P_{\mathrm{S}}(W) = \langle \delta(W - W_{\mathrm{S}}) \rangle, \qquad P_{\mathrm{R}}(W) = \langle \delta(W - W_{\mathrm{R}}) \rangle, \tag{34}$$

where $\langle \cdots \rangle$ stands for the average over trajectories. For an infinite number of pulls, the Crooks fluctuation relation [43] establishes that the probability distributions (34) satisfy the following identity:

$$\frac{P_{\mathrm{S}}(W)}{P_{\mathrm{R}}(-W)} = \exp\left(\frac{W - \Delta G_{X_{\mathrm{min}}}^{X_{\mathrm{max}}}}{k_{\mathrm{B}}T}\right). \tag{35}$$

This relation provides an experimental way to extract the value of $\Delta G_{X_{\mathrm{min}}}^{X_{\mathrm{max}}}$ from measurements of the irreversible work. In particular, the two distributions $P_{\mathrm{S}}(W)$ and $P_{\mathrm{R}}(-W)$ cross each other at the reversible work value, $W = \Delta G_{X_{\mathrm{min}}}^{X_{\mathrm{max}}}$, thus providing a method for deriving the free energy difference between the initial and final states. The reversible work $\Delta G_{X_{\mathrm{min}}}^{X_{\mathrm{max}}}$ gets contributions from pulling the bead and stretching the handles and the ssDNA (see appendix C). In particular, we have defined $\Delta G_1(f_{\mathrm{max}})$ in (C.8) as that part of the reversible work that gets contributions only from unfolding and stretching the hairpin,

$$\Delta G_1(f_{\mathrm{max}}) = \Delta G_{X_{\mathrm{min}}}^{X_{\mathrm{max}}} - \frac{1}{2k_{\mathrm{eff}}}\left[(f_{\mathrm{max}})^2 - (f_{\mathrm{min}})^2\right]. \tag{36}$$

In what follows we subtract for each molecule from the value of the work W the term $(1/(2k_{\mathrm{eff}}))[(f_{\mathrm{max}})^2 - (f_{\mathrm{min}})^2]$ to directly estimate the contribution to the free energy of the hairpin, $\Delta G_1(f_{\mathrm{max}})$. The value of $\Delta G_1(f_{\mathrm{max}})$ can be derived by looking at the crossing of the stretching and releasing work distributions. Although stretching and releasing work distributions for the same molecule taken at different speeds cross at a common value $\Delta G_1(f_{\mathrm{max}})$ (data not shown), work histograms mostly change from molecule to molecule revealing some variability in our estimates for $\Delta G_1(f_{\mathrm{max}})$. This is probably due to the fact that we are using very short tethers as handles which, due to their large rigidity and depending on the angle formed by the tether connecting the two beads, introduce a high variability to the free energy correction $(1/(2k_{\mathrm{eff}}))[(f_{\mathrm{max}})^2 - (f_{\mathrm{min}})^2]$.

In figure 9 (left panel) we show work distributions for three different molecules pulled at different speeds. To better show the systematic dependence of work distributions on the pulling speed, the histograms shown in figure 9 (left panel) have been shifted to make the crossing point (between stretching and releasing distributions) coincide with the value of $\Delta G_1(f_{\mathrm{max}})$ averaged over all molecules (see below and table 3).

In order to validate the fluctuation relation (35) and extract the value of $\Delta G_1(f_{\mathrm{max}})$ for each molecule we have analysed data in two ways:

Bennet acceptance ratio method. The details of this method have been described elsewhere [20, 44]. In a nutshell, Bennett's method consists in defining two functions,

$$z_{\mathrm{S}}(u) = \left\langle g_u(W) \exp\left(-\frac{W}{k_{\mathrm{B}}T}\right)\right\rangle_{\mathrm{R}}, \tag{37a}$$

$$z_{\mathrm{R}}(u) = \log\left(\langle g_u(W)\rangle_{\mathrm{S}}\right), \tag{37b}$$

J. Stat. Mech. (2009) P02060

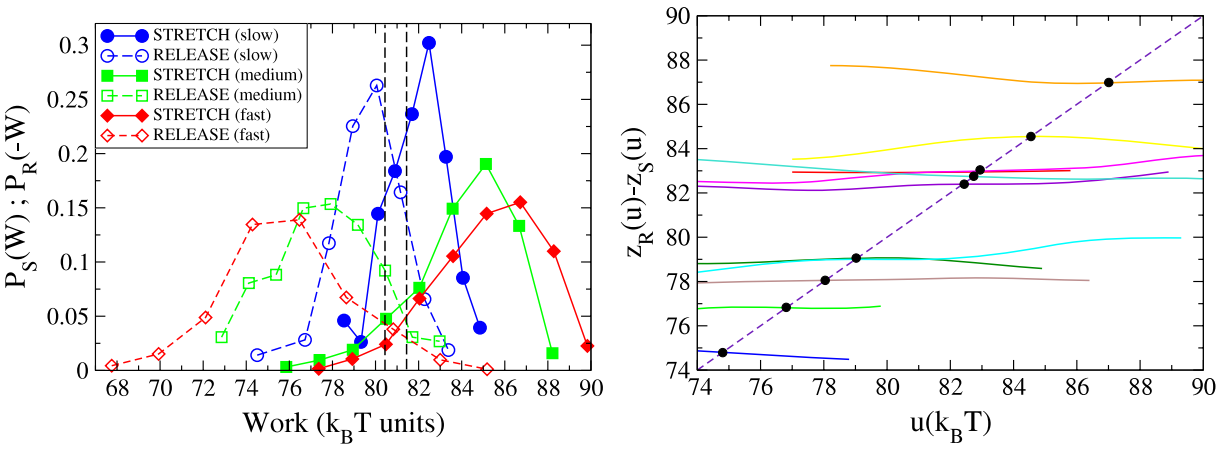

Figure 9. Left: typical work distributions for three molecules at three different loading rates: 1 pN s^{-1} (slow, blue), 4.88 pN s^{-1} (medium, green), 14.9 pN s^{-1} (fast, red). Work values have been shifted in such a way that the crossing between the stretching and releasing work distributions is observed at the average value $\Delta G_1^{\rm FR} = 80.94 k_{\rm B}T$ (see table 3). The vertical lines show the range of experimental error estimated for the value of $\Delta G_1^{\rm FR}$. Right: Bennett acceptance ratio method for extracting the value of $\Delta G_1(f_{\rm max})$ for all 11 molecules (shown as black dots).

Table 3. Mean and standard deviations of free energy parameters obtained from the Crooks fluctuation relation. Averages are taken over 11 different molecules that have been pulled at different pulling speeds: 18.5 nm s^{-1} or 1 pN s^{-1} (1 molecule, 193 cycles), 36.5 nm s^{-1} or 1.95 pN s^{-1} (2 molecules, 160 cycles), 86.2 nm s^{-1} or 4.88 pN s^{-1} (3 molecules, 570 cycles), 156 nm s^{-1} or 8.1 pN s^{-1} (2 molecules, 725 cycles), 274.3 nm s^{-1} or 14.9 pN s^{-1} (3 molecules, 1580 cycles). The value for $\Delta(f^2/2k_{\rm eff})$ depends on the maximum and minimum forces, that vary for each molecule. Therefore we just show the average of this number without giving the error.

$x_{\rm ssDNA}$ (nm)	d_0 (nm)	$(\Delta G_{\rm ssDNA})$ $(k_{\rm B}T)$	$\Delta(f^2/2k_{\rm eff})$ $(k_{\rm B}T)$
23.70(03)	2.0	32.40(04)	341.35
$(\Delta G_1)^{\rm FR}$ $(k_{\rm B}T)$	$(\Delta G_0)^{\rm FR}$ $(k_{\rm B}T)$	$(\Delta G_0)^{\rm FR}$ (kcal mol^{-1})	Mfold (kcal mol^{-1})
80.9(1.0)	58.2(1.0)	34.2(6)	36.81

where $g_u(W)$ is an arbitrary real function that depends on a parameter u and the average $\langle\cdots\rangle_{\rm S\,(R)}$ is taken over the stretching (releasing) process. From (35), it can be proven that

$$z_{\rm R}(u) - z_{\rm S}(u) = \frac{\Delta G_{X_{\rm min}}^{X_{\rm max}}}{k_{\rm B}T}, \tag{38}$$

showing that the difference between the two functions is constant over u and equal to the reversible work. It has been shown by Bennett [45] that the optimal (i.e. minimal variance) estimate of $\Delta G_{X_{\rm min}}^{X_{\rm max}}$ is given by

$$g_\mu(W) = \frac{1}{1 + (N_{\rm S}/N_{\rm R}) \exp\left((W-u)/(k_{\rm B}T)\right)}, \tag{39}$$

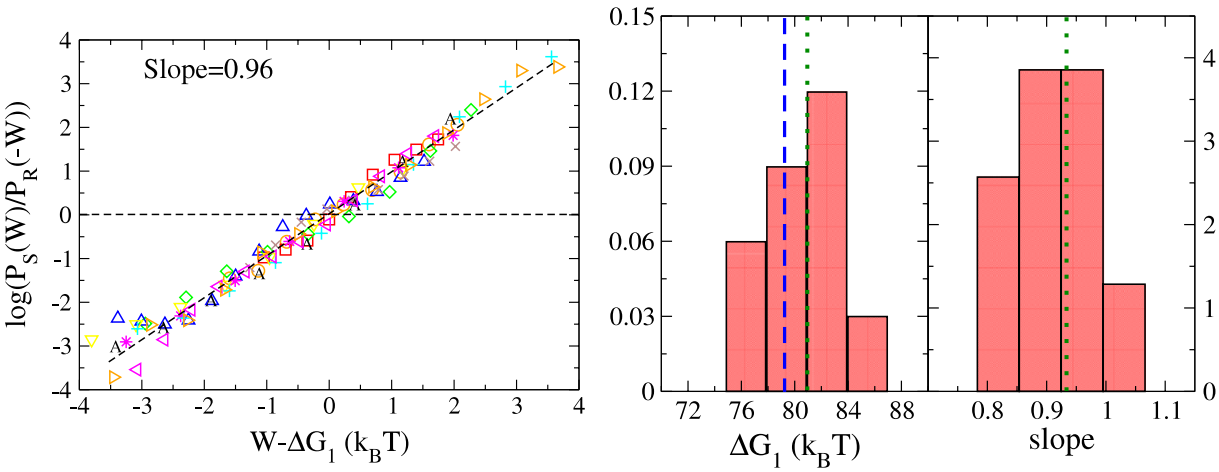

Figure 10. Left: experimental verification of the Crooks fluctuation relation (35). For each molecule, work data have been shifted to cross the horizontal axis (dashed line) at $W = \Delta G_1(f_{\max})$ (corresponding to the black dots shown in figure 9, right panel). Different symbols correspond to the 11 molecules. The continuous line is a weighted linear fit to all data that have slope equal to 0.96. Right: histograms of the values of $\Delta G_1(f_{\max})$ and the slopes corresponding to data shown in the left panel. Statistics collected over 11 molecules. The vertical dotted lines show the mean of the histogram whereas the dashed line in the histogram of $\Delta G_1(f_{\max})$ indicates the average value of ΔG_1 that has been obtained from kinetics (section 5 and table 1).

with $u = \Delta G_{X_{\min}}^{X_{\max}}$. $N_{\mathrm{S\,(R)}}$ stands for the number of pulls during the stretching (releasing) process. The same result has been obtained by Pande and co-workers by using maximum likelihood methods [46]. In figure 9 (right panel) we show the test applied to work data for all molecules. The experimental data for $z_{\mathrm{R}}(u) - z_{\mathrm{S}}(u)$ are approximately constant for each molecule over a wide range of u. The best estimate for $\Delta G_1(f_{\max})$ in (36) is obtained by looking at the intersection of the experimental data with the line $z_{\mathrm{R}}(\mu) - z_{\mathrm{S}}(u) = u/k_{\mathrm{B}}T$ (black dots in the figure). As we can see, the fluctuation relation is validated for each molecule. However there is a strong variability from molecule to molecule for the values $\Delta G_1(f_{\max})$.

Direct representation of the probability ratio. The validity of the fluctuation relation (35) is again observed in figure 10 (left panel) where we have plotted the ratio in the lhs of (35) on a logarithmic scale versus the work W. Like for the work histograms shown in figure 9 (left panel), work values have been shifted for the estimate $\Delta G_1(f_{\max})$ to match the average value $\Delta G_1^{\mathrm{FR}} = 80.94 k_{\mathrm{B}}T$ over all molecules (table 3). Finally, in figure 10 (right panel) we plot the histogram of values for $\Delta G_1(f_{\max})$ obtained for different molecules. As we already saw for the kinetics, the value of $\Delta G_1(f_{\max})$ changes from molecule to molecule, yet the average value $\Delta G_1^{\mathrm{FR}} = 80.94 k_{\mathrm{B}}T$ (table 3) is compatible with the estimate obtained from the kinetics $\Delta G_1 = 78.73$ (section 5 and table 1). In figure 10 (right panel) we also show the histogram of the different slopes of the fluctuation relation shown in the left panel. The fluctuation relation is reasonably well satisfied by the experimental data with an average slope of 0.93. However, if we weight the different slopes according to the number of pulls for each molecule we obtain 0.96, which is closer to the expected value of 1.

J. Stat. Mech. (2009) P02060

7. Derivation of the value of ΔG_0

In the preceding sections we showed ways of extracting the values of ΔG_1 and $\Delta G_{X_{\min}}^{X_{\max}}$ by using rupture force kinetics or the fluctuation relation. Now we face the problem of extracting the value of the free energy of formation of the hairpin at zero force, ΔG_0, using the two methods. As we saw in (15) and (C.9), and in order to extract ΔG_0, we must subtract from the total energy ΔG_1 and $\Delta G_{X_{\min}}^{X_{\max}}$ the stretching contribution to the free energy,

$$G_{\rm ssDNA}(0 \to x^{l_N}; f) = \int_0^{x^{l_N}} F_{\rm ssDNA}^{l_N}(y)\,{\rm d}y, \qquad f = F_{\rm ssDNA}^{l_N}(x_N), \tag{40}$$

with $f = f_{\rm c}$ in (15) and $f = f_{\max}$ in (C.9). $l_N = (2N+L)d$ denotes the full contour length of the hairpin (section 3.1). For the elastic response of the ssDNA, $F_{\rm ssDNA}^{l}(x)$, we use the freely jointed chain model [3, 47],

$$x(f) = l\left(1+\frac{f}{Y}\right)\left[\coth\left(\frac{fb}{k_{\rm B}T}\right) - \frac{k_{\rm B}T}{fb}\right], \tag{41}$$

with l the contour length of the ssDNA, b the Kuhn length and Y the Young modulus. For our temperature and salt conditions we take $b = 1.43$ nm, $Y = 812$ pN [3, 47].

We must stress that in order to extract ΔG_0 from either rupture force kinetics data or by using the fluctuation relation, it is necessary to take into account the fact that the force is not controlled and adopt expressions derived in the appropriate experimental mixed ensemble. In what follows we consider both cases.

Deriving ΔG_0 from rupture force kinetics. From the value obtained for ΔG_1 from rupture force kinetics (table 1), we now adopt the expression (15) with $\Delta G_1(f_{\rm c}) = \Delta G_1$ where ΔG_1 has been measured from kinetics as explained in section 3.3. However, using that expression would lead to incorrect results for ΔG_0. The reason is that in our experiments the force is not controlled, as we only control the position of the trap. As we have shown in appendix C, a contraction in molecular extension (induced by the finite diameter of the hairpin) shifts the free energy of the fully unfolded state, relative to any partially unfolded intermediate state, by an amount equal to $-f_{\rm c}d_0$. Therefore,

$$\Delta G_0 = \Delta G_1 - G_{\rm ssDNA}(0 \to x_N; f_{\rm c}) + f_{\rm c}d_0, \qquad f_{\rm c} = F_{\rm ssDNA}^{l_N}(x_N). \tag{42}$$

Although the values obtained for ΔG_0 show the same dispersion as we saw for ΔG_1 in section 5 (see figure 8), the average value of ΔG_0 is not far from the Mfold [23] predicted value (figure 11 and table 2).

Deriving ΔG_0 from the fluctuation relation. We now use (C.7),

$$\Delta G_0 = \Delta G_1(f_{\max}) - G_{\rm ssDNA}(0 \to x^{l_N}; f_{\max}) + f_{\max}d_0, \tag{43}$$

with $f_{\max}$ the maximum force during the force cycles. We have determined the value of ΔG_0 for each molecule using the values for $\Delta G_1(f_{\max})$ previously determined in section 6.1. As we saw in figure 8, there is also some variability for the values of ΔG_0 obtained for different molecules using this method. However, the average of the different values is not far from the value expected from Mfold [23] (figure 11 and table 2).

J. Stat. Mech. (2009) P02060

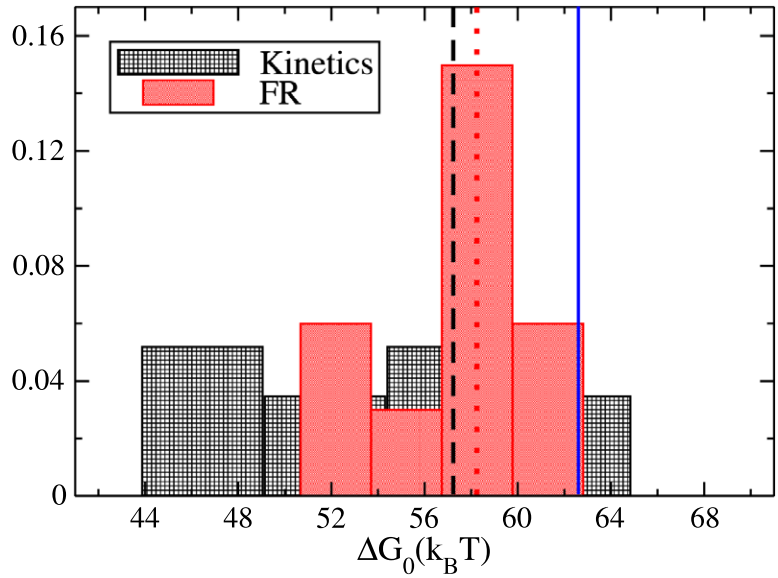

Figure 11. Histograms of the values of ΔG_0 obtained from kinetics (table 2) and the fluctuation relation (table 3). The vertical dashed line indicates the best estimate for ΔG_0 obtained from kinetics (black), the vertical dotted line indicates the best estimate obtained from the fluctuation relation (red) and the vertical continuous line the value predicted by Mfold [23] (blue) at the experimental conditions (23 °C and 1 M NaCl).

8. Conclusions

In this work we have investigated the mechanical unfolding of DNA hairpins using optical tweezers. We have tested the validity of Kramers–Bell theory for force dependent folding/unfolding kinetic rates by comparing theoretical predictions to results from single-molecule pulling experiments on DNA hairpins. We introduced the concept of the free energy landscape for generic nucleic acid (DNA and RNA) molecules and derived simplified expressions for the Kramers–Bell kinetic rates. To validate the theoretical predictions we have carried out experiments on a specifically designed DNA sequence that displays cooperative two-state behaviour. According to the theory, this sequence has a free energy landscape characterized by two states (folded and unfolded) that are separated by a single barrier and a transition state located in a position along the molecular sequence that is independent of the applied force. By doing rupture force measurements we are able to predict the main parameters that characterize the free energy landscape of the hairpin, such as: the distances of the folded and unfolded states from the transition state ($x^{\mathrm{F}}, x^{\mathrm{UF}}$), the free energy difference between the two states (ΔG_1) and the coexistence rate (k_{c}). By measuring the mechanical work and using the Crooks fluctuation relation we can also extract the reversible work in our experiments. Measurements of both types (rupture force kinetics ones and the fluctuation relation ones) yield values for the free energy of formation of the hairpin at zero force, ΔG_0, that are compatible with each other and with the calorimetry based prediction of Mfold. We note the following results:

- *Validity of the Kramers–Bell simplified rates.* The low value of the released molecular extension x_{m} obtained in kinetic studies suggests that the Kramers–Bell model

described in section 3 is an oversimplification of the true folding/unfolding kinetics of the hairpin. It provides estimates for the kinetic parameters that fit the expected values obtained from theory within 15%, but cannot do better. Another possible explanation for such lower values of $x_{\rm m}$ is molecular fraying at the beginning of the hairpin stem that reduces the molecular length and free energy of the hairpin. Given the complexity of the molecules that we are investigating, a 15% agreement between theory and experiment can be considered reasonably good. Yet it would be desirable to explore different sequences and molecular constructions and develop models that can improve the agreement between theory and experiments.

- *Free energy recovery.* A noticeable result from our experiments is the strong variability observed for the parameters extracted from rupture force kinetic studies for different molecules pulled at different speeds (table 1 and figure 8). Variability between parameters is an inherent aspect of single-molecule experiments. As regards the free energy of the hairpin ΔG_0, and as shown in figure 11, the fluctuation relation given by Crooks is compatible with the estimate obtained from rupture force kinetics. Both values are 2–3 kcal mol^{-1} below the value predicted by Mfold leading to a discrepancy between 5 and 10%. Yet the fluctuation relation provides less spread values and more reliable final estimates for ΔG_0. Many sources of error can account for such discrepancies: limitations of the nearest neighbour base pair model used to describe the thermodynamics of unzipping as well as uncertainty in the Mfold nearest neighbour free energies; the inaccurate knowledge of the elastic properties of the released ssDNA; the inaccurate determination of the diameter of the hairpin; molecular fraying; and force calibration and other experimental errors.
- *The diameter of the hairpin d_0 and the elastic properties of the ssDNA.* The value of d_0 ($\simeq$2 nm) taken from structural studies of the double helix, and the polymer model used to model the elastic response of the ssDNA, are particularly important for correctly estimating the value of ΔG_0. For example, a 20% error in the value of d_0 introduces a 1 kcal mol^{-1} error in ΔG_0 ($\simeq 1.6 k_{\rm B}T$ at room temperature). How reliable is our value for d_0? How accurate are the parameters of the freely jointed chain (Kuhn length, Young modulus and interbase distance) for describing the elastic properties of the ssDNA released by the hairpin? It would be very interesting to carry out similar detailed investigations on other DNA sequences. In this way we could check whether the values that we adopted for these parameters are generically accurate for arbitrary hairpin sequences (or instead depend on the DNA sequence).

Two-state models are very useful for addressing questions related to thermodynamics and kinetics of force induced transitions. They guide us in validating and detecting limitations of current theories and models describing the folding of nucleic acids and proteins. Two-state models are also useful for investigating issues related to the irreversibility and dissipation of nonequilibrium small systems as reported in our companion paper [48]. Finally, the current investigation is a first step towards approaching the force induced folding/unfolding kinetics of more complex molecular structures.

Acknowledgments

We acknowledge financial support from grants FIS2007-61433, NAN2004-9348, SGR05-00688.

Appendix A. Free energy landscape in the mixed ensemble

In section 3 we assumed that the experimentally controlled variable is the external force. However, this is far from true in single-molecule experiments with optical tweezers or atomic force microscopy, where the force is a fluctuating variable[5]. Is it possible to define and compute free energy landscapes beyond the force ensemble worked out in section 3? Here we show how to extend the concept of the free energy landscape to the mixed ensemble case relevant for our pulling experiments. The presentation here is summarized; the interested reader will find details in [33].

A schematic representation of the relevant experimental set-up corresponding to the mixed ensemble is shown in figure A.1. Let $X, x_n, x_{\rm b}, x_{\rm h}$ denote the trap–pipette distance, the molecular extension of the hairpin (2), the bead position in the trap and the handle total extension, respectively. These satisfy $X = x_{\rm b} + x_{\rm h} + x_n$. The force is given by $f = k_{\rm b}x_{\rm b}$, where $k_{\rm b}$ is the stiffness of the trap. In the mixed ensemble, the molecular extension of the hairpin plus handles ($\ell_n \equiv x_n + x_{\rm h}$) and the force ($f$) are fluctuating variables and only X is externally controlled. Similarly to what we did in section 3, we let $G(\ell_n, X)$ denote the free energy necessary to break the first n base pairs along the hairpin (starting from the beginning of the fork), thus generating a molecular extension (bead-to-bead) ℓ_n when the trap–pipette distance is equal to X. We can write

$$G(\ell_n, X) = G(\ell_n, 0) + G_{\rm stretch}(0 \to \ell_n; X), \tag{A.1}$$

where $G_{\rm stretch}(0 \to \ell_n; X)$ gets contributions from the bead, the handles and the ssDNA released by the hairpin:

$$G_{\rm stretch}(0 \to \ell_n; X) = G_{\rm b}(0 \to x_{\rm b}; X) + G_{\rm h}(0 \to x_{\rm h}; X) + G_{\rm ssDNA}(0 \to x^{l_n}; X). \tag{A.2}$$

The initial condition $X = 0$ in the term $G(\ell_n, 0)$ in (A.1) must be understood as that position of the trap where all elements are fully relaxed and subject to zero tension. The different terms in (A.2) are given by

$$G_{\rm b}(0 \to x_{\rm b}; X) = \int_0^{x_{\rm b}} F_{\rm b}(y)\,{\rm d}y, \tag{A.3}$$

$$G_{\rm h}(0 \to x_{\rm h}; X) = \int_0^{x_{\rm h}} F_{\rm h}(y)\,{\rm d}y, \tag{A.4}$$

$$G_{\rm ssDNA}(x_0 \to x^{l_n}; X) = \int_0^{x^{l_n}} F^{l_n}_{\rm ssDNA}(y)\,{\rm d}y - F^{l_N}_{\rm ssDNA}(x_N)(1 - \delta_{n,N}), \tag{A.5}$$

where $F_{\rm b}(y) = k_{\rm b}y$ is the elastic response of the bead, $F_{\rm h}(y)$ stands for the equilibrium force–extension curve for the handles and $F^{l_n}_{\rm ssDNA}(y)$ is the equilibrium force–extension curve for the ssDNA of contour length l_n. The last term in (A.5) accounts for the shortening of the molecular extension equal to the diameter of the hairpin that occurs when the last base pair of the hairpin unzips. The contour length l_n in (A.5) satisfies the

[5] Exceptions are for magnetic tweezers [49] or specifically designed tweezers set-ups with zero-stiffness regions [50]. Force feedback systems are not ideal constant force systems as they introduce other sorts of noise effects due to the limited feedback frequency (typically around 1 kHz).

J. Stat. Mech. (2009) P02060

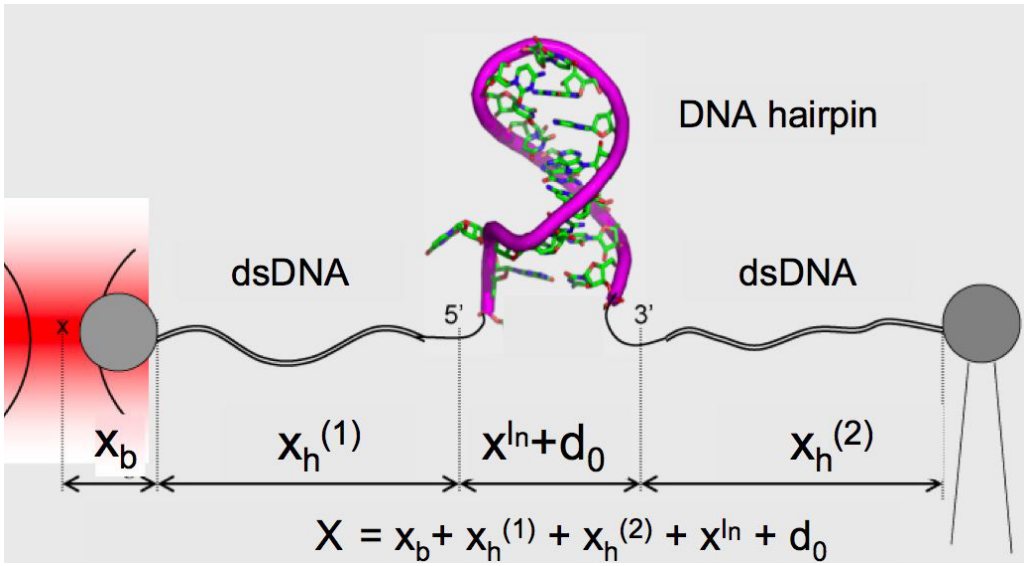

Figure A.1. Schematics of the mixed ensemble. The total distance X is expressed as the sum of the different extensions $x_\mathrm{b}, x_\mathrm{h}, x_n$. $x_\mathrm{h} = x_\mathrm{h}^{(1)} + x_\mathrm{h}^{(2)}$ is the total length of the handles, while the extension x_n has been defined in (2). The hairpin diameter d_0 is taken to be equal to 2 nm and must be included in x_n for all configurations of the hairpin with the exception of the fully unfolded one.

mechanical equilibrium conditions,

$$f = F_\mathrm{b}(x_\mathrm{b}) = F_\mathrm{h}(x_\mathrm{h}) = F^{l_n}_\mathrm{ssDNA}(x^{l_n}), \qquad X = x_\mathrm{b} + x_\mathrm{h} + x^{l_n} + d_0(1 - \delta_{n,N}), \tag{A.6}$$

defining also the Lagrange multiplier f (corresponding to the average of the instantaneous and fluctuating force acting on each element). Note that for a given pair (ℓ_n, X) we have three unknowns $(x_\mathrm{b}, x_\mathrm{h}, x_n)$. The three independent equations in (A.6) fully determine the system so we can exactly compute $G(\ell_n, X)$ as a function of ℓ_n for a given value of X. For that we must know the elastic response of the different elements: $F_\mathrm{b}, F_\mathrm{h}, F^{l}_\mathrm{ssDNA}$.

Appendix B. Dependence of $B_1(f), \Delta G_1(f)$ across the transition

Here we show that terms of the type $G_\mathrm{ssDNA}(0 \to x^{l_\mathrm{F}}; f)$ entering in (10) and (11) vary with f much less than the corresponding product fx^F does. In other words,

$$\frac{\partial G_\mathrm{ssDNA}(0 \to x^{l_\mathrm{F}}; f)}{\partial f} \ll x^\mathrm{F} + f\frac{\partial x^\mathrm{F}}{\partial f}, \tag{B.1}$$

where we assume that x^F generally depends on f (see section 3.1). We start from (4), (1) and write

$$\frac{\partial}{\partial f} G_\mathrm{ssDNA}(0 \to x^{l_\mathrm{F}}; f) = \int_0^{x^{l_\mathrm{F}}} \frac{\partial F^{l_\mathrm{F}}_\mathrm{ssDNA}(y)}{\partial f}\,\mathrm{d}y + f\frac{\partial x^\mathrm{F}}{\partial f}, \tag{B.2}$$

where $F^{l_\mathrm{F}}_\mathrm{ssDNA}(y)$ in the integrand depends on f through the dependence of the contour length as given in (1). The elastic responses of biopolymers (e.g. ssDNA) satisfy either

the worm-like chain model or the freely jointed chain model. In both cases we have that the force is solely a function of the extension divided by the contour length,

$$F^{l}_{\mathrm{ssDNA}}(y) \equiv \hat{F}_{\mathrm{ssDNA}}(y/l). \tag{B.3}$$

It is also reasonable to assume that the relative change in the contour length l_{F} of the released ssDNA is at most equal to the relative change of the distance x^{F},

$$\frac{1}{l_{\mathrm{F}}}\frac{\partial l_{\mathrm{F}}}{\partial f} \leq \frac{1}{x^{\mathrm{F}}}\frac{\partial x^{\mathrm{F}}(f)}{\partial f}. \tag{B.4}$$

From (B.3), (B.4) we can write

$$\frac{\partial F^{l_{\mathrm{F}}}_{\mathrm{ssDNA}}(y)}{\partial f} = \frac{\partial F^{l_{\mathrm{F}}}_{\mathrm{ssDNA}}(y)}{\partial l_{\mathrm{F}}}\frac{\partial l_{\mathrm{F}}}{\partial f} \leq -\frac{y}{x^{\mathrm{F}}}\frac{\partial F^{l_{\mathrm{F}}}_{\mathrm{ssDNA}}(y)}{\partial y}\frac{\partial x^{\mathrm{F}}}{\partial f}. \tag{B.5}$$

Inserting this expression in the integrand in (B.2) and doing an integration by parts we obtain

$$\int_0^{x^{\mathrm{F}}} \frac{\partial F^{l}_{\mathrm{ssDNA}}(y)}{\partial f}\,\mathrm{d}y \leq -\frac{1}{x^{\mathrm{F}}}\frac{\partial x^{\mathrm{F}}}{\partial f}\left(f x^{\mathrm{F}} - \int_0^{x^{\mathrm{F}}} F^{l}_{\mathrm{ssDNA}}(y)\,\mathrm{d}y\right). \tag{B.6}$$

Plugging this expression into (B.2) we get

$$\frac{\partial G_{\mathrm{ssDNA}}(0 \to x^{\mathrm{F}}; f)}{\partial f} \leq \frac{1}{x^{\mathrm{F}}}\frac{\partial x^{\mathrm{F}}}{\partial f}\int_0^{x^{\mathrm{F}}} F^{l}_{\mathrm{ssDNA}}(y)\,\mathrm{d}y \leq f\frac{\partial x^{\mathrm{F}}}{\partial f} \ll x^{\mathrm{F}} + f\frac{\partial x^{\mathrm{F}}}{\partial f}, \tag{B.7}$$

where we introduced the upper bound $F^{l}_{\mathrm{ssDNA}}(y) \leq f$ in the integrand. The last inequality is generally valid for short hairpins that are characterized by a rigid ssDNA where, according to (B.3),

$$k_{\mathrm{ssDNA}} = \frac{\partial f}{\partial x^{\mathrm{F}}} \gg \frac{f}{x^{\mathrm{F}}}. \tag{B.8}$$

Therefore we proved (B.1). The same demonstration applies for the term $G_{\mathrm{ssDNA}}(0 \to x^{l_N}; f)$, proving that we can approximate (16*a*), (16*b*) by the simplified rates (18).

Appendix C. Reversible work in the mixed ensemble

Here we show which terms contribute to the experimentally measured reversible work $\Delta G^{X_{\max}}_{X_{\min}}$ appearing in the Crooks fluctuation relation (35). From the definition of $G(x, X)$ in appendix A, we can write

$$\Delta G^{X_{\max}}_{X_{\min}} = G(x^{\max}_N, X_{\max}) - G(x_0, X_{\min}), \tag{C.1}$$

where $x^{\max}_N$ is the molecular extension of the fully unfolded hairpin at $X = X_{\max}$. From (A.1) to (A.5) we obtain

$$\Delta G^{X_{\max}}_{X_{\min}} = \int_{x^{\min}_{\mathrm{b}}}^{x^{\max}_{\mathrm{b}}} F_{\mathrm{b}}(y)\,\mathrm{d}y + \int_{x^{\min}_{\mathrm{h}}}^{x^{\max}_{\mathrm{h}}} F_{\mathrm{h}}(y)\,\mathrm{d}y + \int_0^{x^{\max}_N} F^{l}_{\mathrm{ssDNA}}(y)\,\mathrm{d}y - f_{\max}d_0 + \Delta G_0, \tag{C.2}$$

where ΔG_0 was defined in (8) and where we have introduced the equilibrium force at the end of the stretching cycle at $X_{\max}$, $f_{\max} = F^{l_N}_{\mathrm{ssDNA}}(x^{\max}_N)$. Note that the correction

term $f_{\max}d_0$ induced by the finite diameter of the hairpin has a different sign in the force ensemble (6). The reason is that, in the force ensemble, an increase in the total distance X of the system (at fixed force f) decreases the total free energy of the system. However, in the mixed ensemble, the same increase in the total distance X (followed by the corresponding drop in the force f) increases the total free energy of the system.

We now introduce the force dependent rigidity of the handles,

$$k_{\rm h}(f) = \left(\frac{\partial F_{\rm h}(y)}{\partial y}\right)_{f=F_{\rm h}(y)}, \tag{C.3}$$

and use (A.6) to change all integration variables in (C.2) to the Lagrange multiplier (force) f. We finally get

$$\Delta G_{X_{\min}}^{X_{\max}} = \int_{f_{\min}}^{f_{\max}} \frac{f\,{\rm d}f}{k_{\rm b}} + \int_{f_{\min}}^{f_{\max}} \frac{f\,{\rm d}f}{k_{\rm h}(f)} + \int_0^{x_N^{\max}} F_{\rm ssDNA}^{l}(y)\,{\rm d}y - f_{\max}d_0 + \Delta G_0, \tag{C.4}$$

where we have written $f_{\max} = F_{\rm ssDNA}^{l_N}(x_N^{\max})$. If the handles are very rigid compared to the rigidity of the trap then $k_{\rm h} \gg k_{\rm b}$ and therefore the sum of the two integrands in the rhs of (C.4) can be approximated by

$$\frac{1}{k_{\rm eff}} = \frac{1}{k_{\rm b}} + \frac{1}{k_{\rm h}(f)}, \tag{C.5}$$

where $k_{\rm eff}$ is taken as constant in the interval $[f_{\min}, f_{\max}]$. The condition $k_{\rm h} \gg k_{\rm b}$ is reasonably well satisfied in our experiments where we use 29-bp handles. Therefore, by substituting (C.5) and defining

$$\begin{aligned}\Delta G_1(f_{\max}) &= \Delta G_{X_{\min}}^{X_{\max}} - \int_{f_{\min}}^{f_{\max}} \frac{f\,{\rm d}f}{k_{\rm b}} - \int_{f_{\min}}^{f_{\max}} \frac{f\,{\rm d}f}{k_{\rm h}(f)} \\ &= \Delta G_{X_{\min}}^{X_{\max}} - \frac{1}{2k_{\rm eff}}\left((f_{\max})^2 - (f_{\min})^2\right),\end{aligned} \tag{C.6}$$

we get

$$\Delta G_1(f_{\max}) = \int_0^{x_N^{\max}} F_{\rm ssDNA}^{l}(y)\,{\rm d}y - f_{\max}d_0 + \Delta G_0, \qquad f_{\max} = F_{\rm ssDNA}^{l_N}(x_N^{\max}). \tag{C.7}$$

Note that the expression (C.6) for $\Delta G_1(f_{\max})$ is the equivalent of (10) in the force ensemble. According to (C.7) it only depends on the maximum force at which the molecule is unfolded; therefore we explicitly indicate such dependence of ΔG_1 in its argument. Using (C.6), (C.7) it is possible to extract ΔG_0 from the knowledge of $\Delta G_{X_{\min}}^{X_{\max}}, f_{\min}, f_{\max}$ and the elastic properties of the ssDNA:

$$\Delta G_{X_{\min}}^{X_{\max}} = \frac{1}{2k_{\rm eff}}\left((f_{\max})^2 - (f_{\min})^2\right) + \Delta G_1(f_{\max}), \tag{C.8}$$

$$\Delta G_0 = \Delta G_{X_{\min}}^{X_{\max}} - \frac{(f_{\max})^2 - (f_{\min})^2}{2k_{\rm eff}} - G_{\rm ssDNA}(0 \to x_N; f_{\max}) + f_{\max}d_0. \tag{C.9}$$

J. Stat. Mech. (2009) P02060

References

[1] Ritort F, 2006 *J. Phys.: Condens. Matter* **18** R531 [arXiv:cond-mat/0609378]
[2] Hormeño S and Arias-González J R, 2006 *Biol. Cell* **98** 679
[3] Smith S B, Cui Y and Bustamante C, 1996 *Science* **271** 795
[4] Wang M D, Yin H, Landick R, Gelles J and Block S M, 1997 *Biophys. J.* **72** 1335
[5] Dessinges M-N, Maier B, Zhang Y, Peliti M, Bensimon D and Croquette V, 2002 *Phys. Rev. Lett.* **89** 248102
[6] Rief M, Gautel M, Oesterhelt F, Fernandez J M and Gaub H E, 1997 *Science* **276** 1109
[7] Liphardt J, Onoa B, Smith S B, Tinoco I Jr and Bustamante C, 2001 *Science* **292** 733
[8] Fernandez J M, Chu S and Oberhauser A F, 2001 *Science* **292** 653
[9] Leger J F, Robert J, Bourdieu L, Chatenay D and Marko J F, 1998 *Proc. Nat. Acad. Sci.* **95** 12295
[10] Yin H, Wang M D, Svoboda K, Landick R, Block S M and Gelles J, 1995 *Science* **270** 1653
[11] Finer J T, Simmons R M and Spudich J A, 1994 *Nature* **368** 113
[12] Noji H, Yasuda R, Yoshida M and Kinosita K Jr, 1997 *Nature* **386** 299
[13] Strick T R, Croquette V and Bensimon D, 2000 *Nature* **404** 901
[14] Abbondanzieri E A, Greenleaf W J, Shaevitz J W, Landick R and Block S M, 2005 *Nature* **438** 460
[15] Wen J-D, Lancaster L, Hodges C, Zeri A-C, Yoshimura S H, Noller H F, Bustamante C and Tinoco I Jr, 2008 *Nature* **452** 598
[16] Woodside M T, Anthony P C, Behnke-Parks W M, Larizadeh K, Herschlag D and Block S M, 2006 *Science* **314** 1001
[17] Woodside M T, Behnke-Parks W M, Larizadeh K, Travers K, Herschlag D and Block S M, 2006 *Proc. Nat. Acad. Sci.* **103** 6190
[18] Bustamante C and Smith S B, 2006 *US Patent Specification* 7,133,132, B2
[19] Smith S B, Cui Y and Bustamante C, 2003 *Methods Enzymol.* **361** 134
[20] Ritort F, 2008 *Adv. Chem. Phys.* **137** 31
[21] SantaLucia J Jr, 1998 *Proc. Nat. Acad. Sci.* **95** 1460
[22] SantaLucia J Jr and Hicks D, 2004 *Annu. Rev. Biophys. Biomol. Struct.* **33** 415
[23] Zuker M, 2003 *Nucleic Acids Res.* **31** 3406
[24] Cocco S, Monasson R and Marko J, 2001 *Proc. Nat. Acad. Sci.* **98** 8608
[25] Cocco S, Monasson R and Marko J, 2002 *Phys. Rev.* E **65** 041907
[26] Bell G I, 1978 *Science* **200** 618
[27] Tinoco I Jr, 2004 *Annu. Rev. Biophys. Biomol. Struct.* **33** 363
[28] Manosas M, Junier I and Ritort F, 2008 *Phys. Rev.* E **78** 061925
[29] Leffer J E, 1953 *Science* **117** 340
[30] Hyeon C and Thirumalai D, 2005 *Proc. Nat. Acad. Sci.* **102** 6789
[31] Hyeon C and Thirumalai D, 2006 *Biophys. J.* **90** 3410
[32] Manosas M, Collin D and Ritort F, 2006 *Phys. Rev. Lett.* **96** 218301 [arXiv:cond-mat/0606254]
[33] Manosas M and Ritort F, 2005 *Biophys. J.* **88** 3224 [arXiv:cond-mat/0405035]
[34] Evans E and Ritchie K, 1997 *Biophys. J.* **72** 1541
[35] Schlierf M and Rief M, 2006 *Biophys. J.* **90** L33
[36] Shillcock J C and Seifert U, 1996 *Phys. Rev.* E **57** 7301
[37] Hummer G and Szabo A, 2003 *Biophys. J.* **85** 5
[38] Gerland U, Bundschuh R and Hwa T, 2001 *Biophys. J.* **81** 1324 [arXiv:cond-mat/0101250]
[39] Gerland U, Bundschuh R and Hwa T, 2003 *Biophys. J.* **84** 2831 [arXiv:cond-mat/0208202]
[40] Wen J D, Manosas M, Li P T X, Smith S B, Bustamante C, Ritort F and Tinoco I Jr, 2007 *Biophys. J.* **92** 2996
[41] Manosas M, Wen J D, Li P T X, Smith S B, Bustamante C, Tinoco I Jr and Ritort F, 2007 *Biophys. J.* **92** 3010
[42] Hyeon C, Morrison G and Thirumalai D, 2008 *Proc. Nat. Acad. Sci.* **105** 9604
[43] Crooks G E, 1999 *Phys. Rev.* E **60** 2721 [arXiv:cond-mat/9901352]
[44] Collin D, Ritort F, Jarzynski C, Smith S B, Tinoco I Jr and Bustamante C, 2005 *Nature* **437** 231
[45] Bennett C H, 1976 *J. Comput. Phys.* **22** 245
[46] Shirts M R, Bair E, Hooker G and Pande V S, 2003 *Phys. Rev. Lett.* **91** 140601
[47] Huguet J M, Forns N, Bizarro C V, Smith S B, Bustamante C and Ritort F, 2009 unpublished
[48] Manosas M, Mossa A, Forns N, Huguet J M and Ritort F, *Dynamic force spectroscopy of DNA hairpins: II. Irreversibility and dissipation*, 2009 *J. Stat. Mech.* P02061
[49] Gosse C and Croquette V, 2002 *Biophys. J.* **82** 3314
[50] Greenleaf W J, Woodside M T, Abbondanzieri E A and Block S M, 2005 *Phys. Rev. Lett.* **95** 208102

J. Stat. Mech. (2009) P02060